Engineered Science
DOI: https://dx.doi.org/10.30919/es8d869

Modelling and Prediction of Machining Forces During End Milling of Glass Fibre Reinforced Polymer Composites Using Regression Analysis and Artificial Neural Networks (ANN)

M. P. Jenarthanan,[1,*] B. Harinesh[1] and U. Arunachalam[2]

Abstract

The objective of this work is to highlight the modelling capabilities of artificial intelligence techniques for predicting the machining force during endmilling of GFRP composites. The present scenario demands such types of models to investigate the influence of the milling parameters on the thrust force during milling operation. In order to predict the performance of the input parameters (feed rate, speed, fibre orientation and depth of cut) and their interactions, detailed experiments were conducted based on the Response Surface Methodology (RSM) and the influences on the thrust force was assessed. The results indicated that the feed rate is the cutting parameter which has greater influence on Machining force for GFRP composite materials, followed by the cutting speed. The developed second order response surface model was validated using confirmation test and the error was found to be within ±0.3%. A Back Propagation (BP) model in Artificial Neural Networks (ANN) was developed. The developed ANN model was compared with the RSM models for the prediction of machining force of milled GFRP composites.

Keywords: FRP composites; Design of Experiments; Artificial intelligence; Machining force; ANN.
Received: 23 March 2022; Revised: 11 April 2023; Accepted: 25 April 2023.
Article type: Research article.

1. Introduction

One of the most crucial machining operations in the production of FRP parts is milling. However, milling of FRPs is done at a much smaller scale than milling of metals, which is characterised by high material removal rates. This is because FRP components are often manufactured close to net shape, and any further milling is mostly used for deburring, trimming, and obtaining contour shape precision.[1] Glass Fibre Reinforced Plastics (GFRP) composite is considered to be an economic alternative to various heavy exotic materials. It is widely used in a variety of applications from aircraft to machine tools due to their light weight, high modulus, specific strength and high fracture toughness.[2] The machining of composite is different from the conventional machining of metal due to the composite's anisotropic and non-homogeneous nature.[3]

Machining force is a property that can affect dimensional accuracy, mechanical item performance, and production costs. Due to these factors, research and development have been conducted with the aim of optimising cutting conditions in order to produce a predetermined machining force.[4] For achieving the desired machining force, it is necessary to understand the mechanisms of the material removal, and the kinetics of machining processes affecting the performance of the cutting tool.[5] When GFRP composites are machined, it is clearly seen that the fibres are cut across and along their lay direction, leaving deformed projections and partially disclosed fibres on the machined surface.[6] Few other experiments were conducted to evaluate the cutting parameters (cutting velocity and feed rate) related to machining force, delamination factor, surface roughness and international dimensional precision in two GFRP composite materials (Viapal VUP 9731 and ATLAC 382-05). Experiments were conducted using design of experiments (full factorial design) to assess the influence of machining parameters on the turning of GFRP composites.[7,8] They concludedthat feed rate is the factor, which has greater influence on machining force, followed by cutting speed. Studies have been done to view how the fibre orientation influence both the quality of the machined surfaces and tool wear.[9] The machinability of composite materials is

[1] *School of Mechanical Engineering, SASTRA Deemed to be University, Thanjavur 613401, Tamil Nadu, India.*
[2] *Mechanical Engineering Department, University College of Engineering, Nagercoil 629004, Tamil Nadu, India.*
**Email:* jenarthanan@mech.sastra.edu (M. P. Jenarthanan)

influenced by the type of fibre embedded in the composites, and more particularly by the mechanical properties. On the other hand, the selection of cutting parameters and the cutting tool are dependent on the type of fibre used in the composites and which is very important in the machining process. In order to know surface quality and dimensional properties, it is necessary to employ theoretical models for prediction purpose. For prediction, the response surface method (RSM) is practical, economical and relatively easy for use.[10] A mathematical and statistical strategy for modelling and analysing situations with the aim of optimising the replies is called response surface methodology. It is a method for constructing and improving empirical models through sequential experimentation. It is possible to create a model of the response to a few independent input variables by running trials and using regression analysis. A point that is close to the ideal can be determined using the response model. Input control relationships that affect responses can be identified and represented by RSM as a two- or three-dimensional hyper surface. The instance where there is only one interesting response has received the majority of attention in RSM. In this case, surface roughness of optimum conditions on the input variables would require simultaneous consideration of all the responses. This is called a multi response problem.[11] To date, several approaches have been proposed for Multi Response Optimization (MRO) including the desirability function approach and loss function approach.[12-14] A number of investigations using RSM are carried out to determine the significant factors affecting the response.[15-17] Recently there has been a lot of interest to develop models for investigating the influence of machining parameters (cutting speed, tool geometry, *etc*.) on response parameters (cost, roughness, time *etc*.) using artificial intelligence techniques.[18-21] The effect of cutting parameters on cutting temperature, vibration (g), surface roughness (Ra), and noise (N) in the turning of AISI P20 die steel using coated tungsten carbide cutting tools is investigated. Experiments were carried out using the Taguchi L18 experimental design with cutting tools with two different types of coatings (CVD and PVD), three different cutting speeds (100,150 and 200m/min), three different feed rates (0.1, 0.15 and 0.2 mm/rev), and a constant cutting depth (1mm).[22] The effects of machining parameters on the experimental and statistical results using the electric discharge method in the machining of AISI D2 cold work tool steel. The design of the experiment was established using the Taguchi *L*18 method. The effect of the experiment parameters on the performance characteristics was analyzed by analysis of variance (ANOVA).[23] Turning tests for AA 6061 alloy with uncoated and PVD-TiB2 coated cutting inserts have been conducted on a CNC turning under dry cutting conditions based on Taguchi L18 (21 × 33) array. Kistler 9257A type dynamometer and equipment have been used in measuring the main cutting force (Fc) in turning experiments. Analysis of Variance (ANOVA) has been applied to define the effect levels of the turning parameters on Fc and Ra. The results indicated that the best performance in terms of Fc and Ra was obtained at an uncoated insert, cutting speed of 350 m/min, feed rate of 0.1 mm/rev, and depth of cut of 1 mm. Moreover, the feed rate is the most influential parameter on Ra and Fc, with 64.28% and 54.9%, respectively. The developed mathematical models for cutting force (Fc) and surface roughness (Ra) present reliable results with coefficients of determination (*R*2) of 96.04% and 92.15%, respectively.[24] In the present work, a mathematical model has been developed to predict the machining force on GFRP materials using response surface method. The "Design Expert 12.0" software is used for regression and graphical analysis of the data collected. The study of effect of cutting parameters on the machining force is done by analyzing the response surface contour plots. Analysis of Variance (ANOVA) is used to check the validity of the model and for finding the significant parameters. Back Propagation (BP) based Artificial Neural Networks (ANN) model was developed to study the Machinability of GFRP composite during endmilling. The developed ANN model was compared with the RSM models for the prediction of machining force of milled GFRP composites.

2. Material, process parameters and measurements

Seven Mill Glass fibre-cloth and epoxy (LY 556) along with hardener (HY 951) were used toprepare the GFRP laminates by Hand lay-up method as shown in Fig. 1. The wide range of properties and its light weight has made GFRP and major asset in Manufacturing. Few of those properties are listed in Table 1. GFRP Laminates are of 300 × 300 × 3 mm thick with the 12 lay-upand 0/90°fibre orientation was used for the milling operation which is similar to that as shown in Fig. 1.

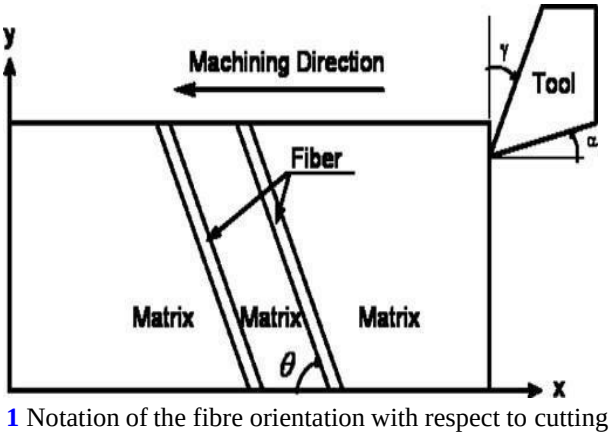

Fig. 1 Notation of the fibre orientation with respect to cutting tool movement.[20]

The cutting tool is made up of solid carbide coated with polycrystalline diamond (PCD) of 3mm diameter as shown in Fig. 2.

Using the CNC milling machine, the experiments are carried out based on the Taguchi L9 (34) orthogonal array. To forecast the impact of each component on the response, Box-Behnken design was used to plan the tests for each parameter.

Table 1. Material properties for the GFRP plates.

Sample No.	Fibre Orientation, (deg)	Tensile strength, (MPa)	Tensile modulus, (GPa)	Shear strength, (MPa)
1	15	153	8.164	7.513
2	30	112	12.100	8.127
3	60	109	12.475	11.054
4	90	229	14.412	12.27
5	120	133	11.569	11.014

Each factor had 2° of freedom. Hence, six was the summation of total degrees of freedom of each factor. The CNC milling machine is automated machinery, and its specifications are given in Table 2.

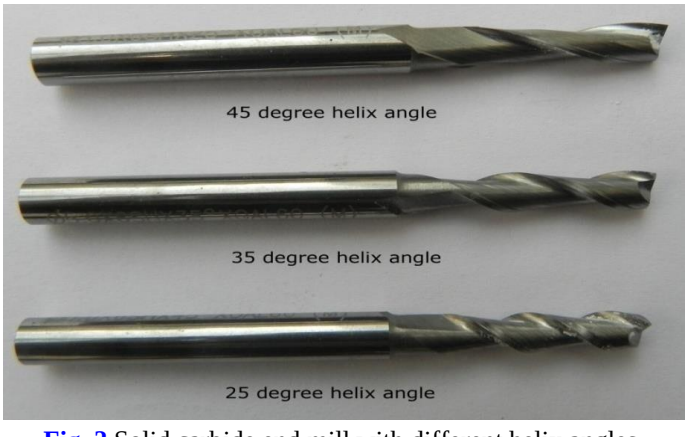

Fig. 2 Solid carbide end mill with different helix angles.

Table 2. Specification of the CNC milling machine.

Type of machine	Vertical machine centre
Make	Hass-Us(Brand New)
Specification	Hass No. 3 Machine
Power	25 KW
Maximum speed	12,000 RPM
X axis	1016 mm
Y axis	520 mm
Z axis	508 mm
Table width	520 x 1200

The fixation of the composite material is as shown in Fig. 3, to make sure that vibrations and displacement are eliminated. Machining force on the work piece is an important attribute of quality in any machining operation. During machining, many factors like feed, speed, depth of cut affect the machining force.

A detailed analysis has been carried out to set the lower and upper limits of the machining factors. The study identifies the maximum and lower bounds of the components. Previous research suggested that when cutting speed increases, so does the machining force. However, it was discovered that very high cutting speeds resulted in a significant amount of glass fibre deformation and surface roughness, so the cutting speed was restricted to between 50 and 100 m/min. Compared to cutting speed and feed rate, the depth of cut has a much smaller impact on the composite machining process, although it still has a sizable impact.[18] The cut depth is regulated at 0.05 to 0.25 mm. Feed rate is the main parameter, which affect the machining process. The increase in feed rate increases the chatter and it produces incomplete machining at a faster traverse, which led to higher surface Machining force and hence low limit of feed rates are advisable in machining GFRP composites. In the present study, the feed rate is selected between 0.04 and 0.12 mm/rev.[19] The identified parameters and its lower and upper limits are given in Table 3.

Table 3. Process control parameters and their limits.

				Levels		
Process parameters	Units	Notation	Variable	-1	0	1
Feed rate	mm/rev	f	A	0.04	0.08	0.12
Cutting speed	m/min	v	B	50	75	100
Depth of cut	mm	d	C	0.05	0.15	0.25

3. Measurements

The output response considered in this study is machining force (Fm). The measurement and calculation of response based on the input parameters are described below.

3.1 Machining force

Force measurement in manufacturing, especially in machining, is very important. This is because:

Force measurement can be used for monitoring the tool conditions, and avoiding breakage during the machining process. It helps us understand machining process,because cutting force is one of the most sensitive indicators of machining performance. Both the static and dynamic components of the cutting force contain information concerning the state of chipformation and the cutting tool. Force measurement enables engineer to optimize manufacturing process and design proper machining tool.

The force measurement was carried out using a Kistler dynamometer. The data acquisition was carried out by appropriate software called Dynawarekistler. The value of machining force in the work piece is determined using the Eq. (1).

$$F_m = \sqrt{(F_x{}^2 + F_y{}^2 + F_z{}^2)} \quad (1)$$

3.2 Response surface methodology and experimental design

Response Surface Methodology (RSM) is a collection of mathematical and statistical techniques that are useful for modelling and analysing of problems in which an output or response influenced by several variables and the goal is to find the correlation between the response and the variables. The steps involved in RSM technique are as follows: (i) designing

Fig. 3 Fixation of GFRP composite plate by using clamps in the machining centre.

a set of experiments for adequate and reliable measurement of the true mean response of interest, (ii) determination of mathematical model with best fits, (iii) finding the optimum set of experimental factors that produces maximum or minimum value of response, and (iv) representing the direct and interactive effects of process variables on the best parameters through two dimensional and three-dimensional graphs. If all variables are assumed to be measurable, the response surface can be expressed as follows Eq. (2):

$$y = f(x_1, x_2, \ldots, x_k) \quad (2)$$

The goal is to optimize the response variable y. It is assumed that the independent variables are continuous and controllable by experiments with negligible errors. It is required to find a suitable approximation for the true functional relationship between independent variables and the response surface. Usually a second-order model (Eq. (3)) is utilized in response surface methodology.

$$y = \beta_0 + \sum_{i=1}^{k} \beta_i x_i + \sum_{i=1}^{k} \beta_{ii} x_i^2 + \sum_{i=1}^{k} \beta_{ij} x_i x_j + \varepsilon \quad (3)$$

where ε is a random error, β is the coefficients, which should be determined in the second- order model, are obtained by the least square method. Owing to slightly wider ranges of the factors, it was decided to use a three-level face- centered central composite design to optimize the experimental conditions. Face-centered central composite designs of second order have been found to be the most efficient tool in RSM to establish the mathematical relation of the response surface using the smallest possible number of experiments without losing its accuracy. In the present case, the size of the experiment is 20 for three machining parameters shown in Table 4.

Table 4. The layout of Box-Behnken composite design with results.

Sl. No	Coded variables			Uncoded variables			Machining force N
Run	A	B	C	f	v	d	Fm
1	0	0	0	0.08	75	0.15	17.628
2	0	0	0	0.08	75	0.15	17.628
3	-1	0	-1	0.04	75	0.05	17.127
4	1	0	-10	0.12	75	0.05	17.811
5	1	-1	0	0.12	50	0.15	18.001
6	0	0	0	0.08	75	0.15	17.628
7	0	0	0	0.08	75	0.15	17.628
8	0	0	1	0.08	75	0.15	17.628
9	0	1	0	0.08	100	0.25	17.798
10	0	0	0	0.08	75	0.15	17.628
11	1	1	0	0.12	100	0.15	18.218
12	-1	1	0	0.04	100	0.15	17.208
13	-1	0	1	0.04	75	0.25	17.418
14	1	0	1	0.12	75	0.25	17.948
15	0	-1	1	0.08	50	0.25	18.676
16	0	-1	-1	0.08	50	0.05	17.541
17	0	0	0	0.08	75	0.15	17.628
18	0	1	1	0.08	100	0.05	17.541
19	0	0	0	0.08	75	0.15	17.628
20	-1	-1	0	0.04	50	0.15	17.208

To simplify the calculation the natural values of input

parameters are converted into coded values. The coded numbers for the variables used in tables are obtained from the following transformation Eq. (4):

$$Xi = \frac{[2X - Xmax + Xmin]}{[\frac{Xmax - Xmin}{2}]} \quad (4)$$

where, X_{max} is the upper level of the parameter, X_{min} is the lower level of the parameter and X_i is the required coded values of the parameter of any value of X from X_{min} to X_{max}.

4. Results and discussions

One of the most important limitations for the choice of machines and cutting parameters in process planning is machining force. For a specific machine tool and work piece setup, the cutting parameters such as feed rate, cutting speed, depth of cut, *etc*., have the greatest influence on the study of machining force characteristics of GFRP composites. The fit summary recommended that the quadratic model is statistically significant for analysis of Machining force. The result of the quadratic model for Machining force in the form of ANOVA is given in the Table 4.

The value of R^2 and adjusted R^2 for Machining force are 96.66% and 93.65% respectively. This means that regression model provides an excellent explanation of the relationship between the independent factors and the responses. The associated *p* value for the model is lower than 0.001 which shows that the model is considered to be statistically significant. Further, factors Feed (A), Speed (B), Depth of cut (C) have significant effects on machining force. The result shows that the feed rate is more significant parameter for the machining force, when compared with the cutting seed, and depth of cut because of higher *F* value. The other model terms are said to be insignificant. It is claimed that the other model terms are unimportant. The lack of fit was found to be very less than $F_{0.01}$ (9, 10) in the present research study and, hence the developed model may be accepted. Final equations from RSM in terms of coded factors and in terms of actual factors are shown in Eq. (5) and Eq. (6) respectively.

Final Equation in Terms of Coded Factors:

$$\sqrt{(\text{Machining Force})} = +4.15 + 1.04 * A - 1.844E{-}003 * B + 0.23 * C + 6.374E{-}003 * A * 1.18 * A * C + 1.448E{-}003 * B * C - 1.36 * A^2 + 8.780E{-}006 * B^2 - 0.42 * C^2 \quad (5)$$

Final Equation in Terms of Actual Factors:

$$\sqrt{(\text{Machining Force})} = +4.14705 + 1.03916 * \text{Feed} - 1.84425E{-}003 * \text{Speed} + 0.23366 * \text{Depth of cut} + 6.37409E{-}003 * \text{Feed} * \text{Speed} - 1.17561 * \text{Feed} * \text{Depth of cut} + 1.44841E{-}003 * \text{Speed} * \text{Depth of cut} - 1.36178 * \text{Feed}^2 + 8.77975E{-}006 * \text{Speed}^2 - 0.41969 * \text{Depth of cut}^2 \quad (6)$$

The experimental values are analyzed using Response Surface analysis and the following relation has been established for Machining force of GFRP composites. Fig. 4 shows the correlation between the predicted and experimental values for Machining force of GFRP composites.

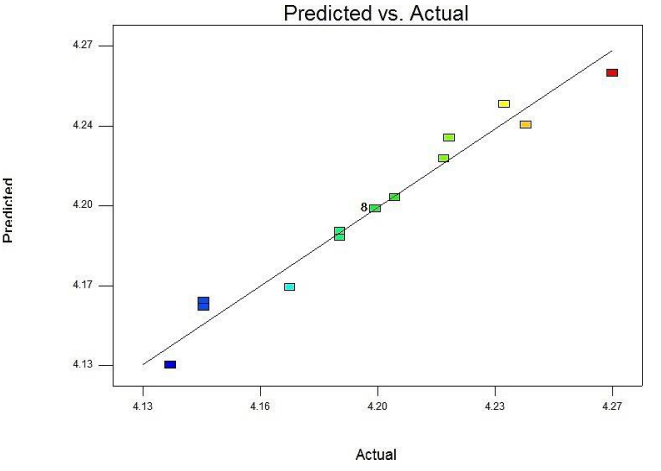

Fig. 4 Graph showing the relationship between the actual and the predicted process.

The influence of different cutting parameters on machining of GFRP composites are studied by using response graph and response table. The influence of parameters on Machining force is shown in as contour figures as Fig. 5, Fig. 6 and Fig. 7.

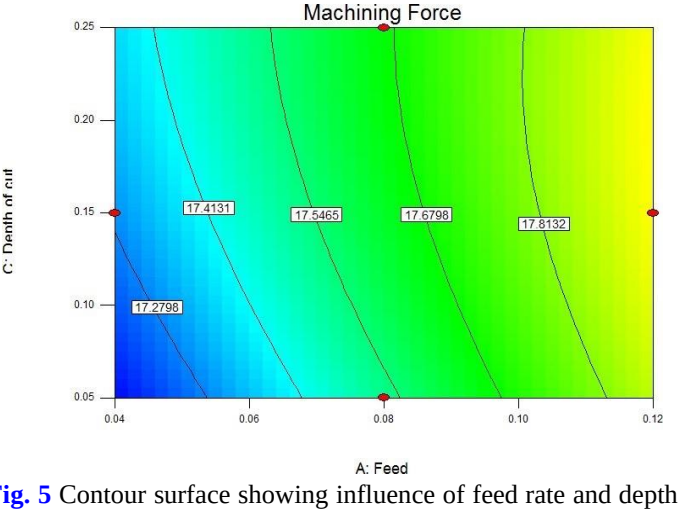

Fig. 5 Contour surface showing influence of feed rate and depth of cut on machining force.

From the figures itis observed that machining force value increases with increase of feed rate, cutting speed and depth of cut. These contour data and the ANOVA result, which is depicted in Table 5, indicate that feed rate, followed by cutting speed and depth of cut, is the primary factor influencing the machining force. This is because a faster feed rate caused more heat to be produced, which in turn caused more tool wear and a rougher surface.[1]

As the feed rate increased, clatter also increased, leading to incomplete machining at a faster traverse and a rise in surface roughness. This is consistent with the results from the study quoted above.[7]

The Fig. 8, Fig. 9 and Fig. 10 show the estimated response surface for the force in relation to the individual parameters of the feed rate, speed and depth of cut.

Table 5. RSM-ANOVA analysis.

Source	Sum of Squares	Df	Mean Square	F Value	p-value Prob>F
Model	0.018	9	2.006 E-003	32.13	<0.0001 (Significant)
A- Speed	2.684E-004	1	2.684 E-004	4.30	0.0649
B-Speed	2.223 E-004	1	2.223 E-004	3.56	0.0885
C- Depth of cut	1.022 E-004	1	1.022 E-004	1.64	0.2297
AB	1.625 E-004	1	1.625 E-004	2.60	0.1377
AC	8.845 E-005	1	8.845 E-005	1.42	0.2614
BC	5.245 E-005	1	5.245 E-005	0.84	0.3809
A2	2.170 E-005	1	2.170 E-005	0.35	0.5685
B2	1.377 E-004	1	1.377 E-004	2.20	0.1684
C2	8.052 E-005	1	8.052 E-005	1.29	0.2826
Residual	6.243 E-004	10	6.243 E-005		
Lack of fit	6.243 E-004	3	2.081 E-004		
Pure error	0.000	7	0.0000		
Cor Total	0.019	19			

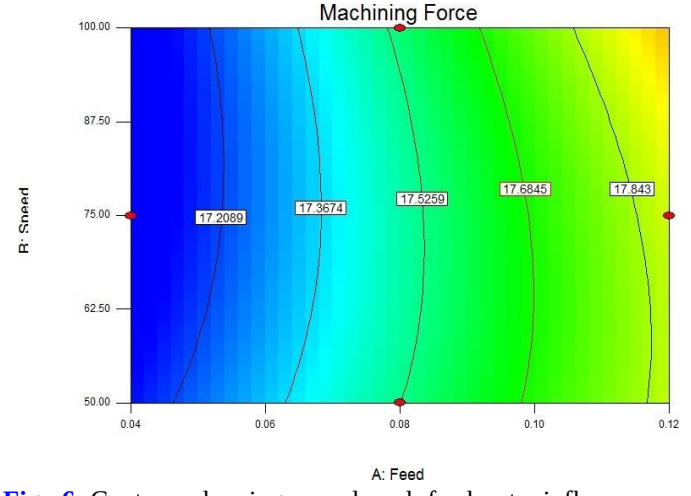

Fig. 6 Contour showing speed and feed rate influences on machining force.

As it seen from these figures, the machining force tends to increase steadily with an increase in feed rate. This is due to the increase in the feed rate causes a sharp rise in the feed force which in turn causes higher friction and produces more damage on the surface. From Table 5, the model indicates the percentage contribution of Feed is higher with an F value of 4.30. It is seen that the cutting speed has been less significant

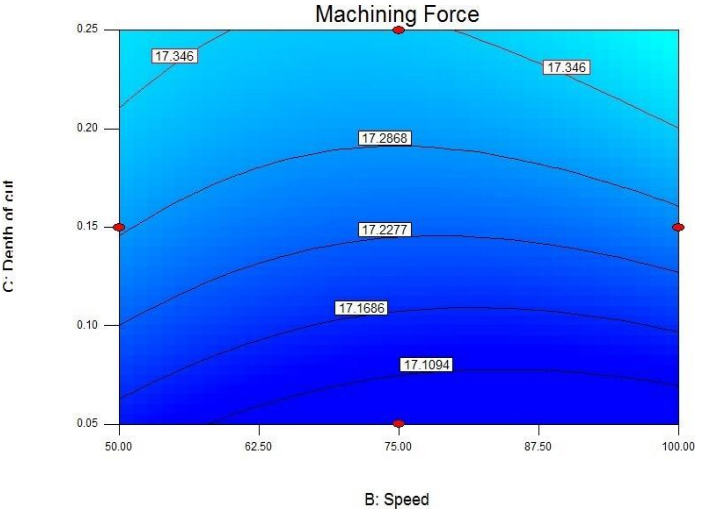

Fig. 7 effect of depth of cut and speed on machining force.

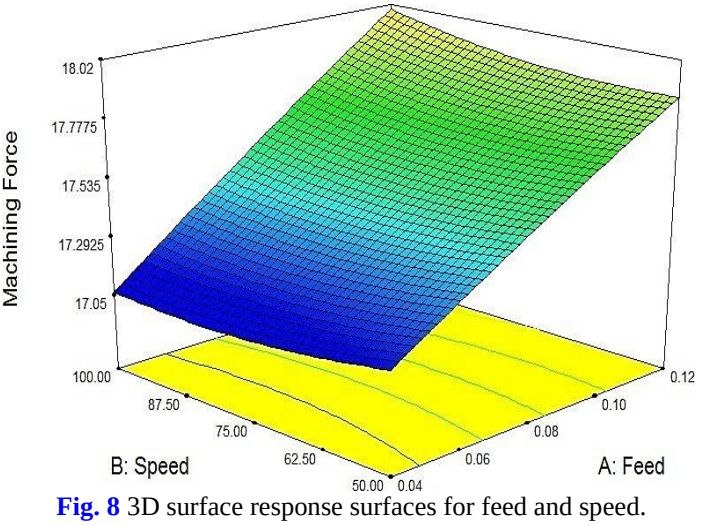

Fig. 8 3D surface response surfaces for feed and speed.

on Machining force when compared with the Feed rate. When the cutting speed ranges between 50 and 100 m/min and the feed rate from 0.04 to 0.12 mm/rev, the machining force value lies within 17.127 to 18.218N. Further, it is also seen that while the cutting speed is between 50 and 100 m/min and the feed rate in the range of 0.04 and 0.12 mm/rev, the Machining force appears to rise from 17.2089 to 17.843 N.

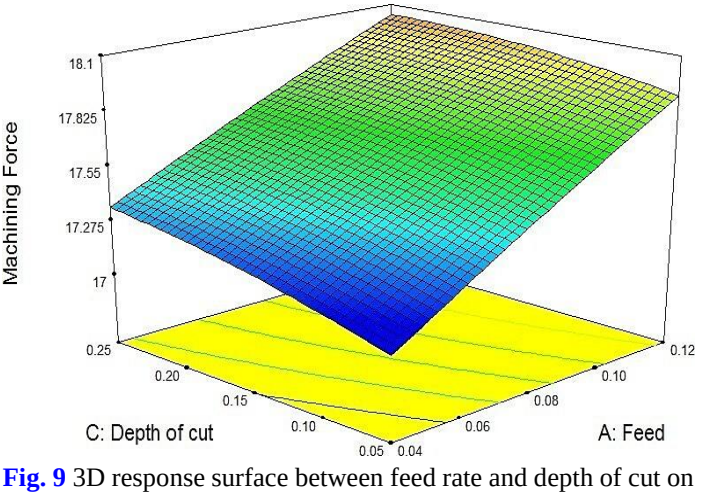

Fig. 9 3D response surface between feed rate and depth of cut on machining force.

Table 5. RSM-ANOVA analysis.

Source	Sum of Squares	Df	Mean Square	F Value	p-value Prob>F
Model	0.018	9	2.006 E-003	32.13	<0.0001 (Significant)
A- Speed	2.684E-004	1	2.684 E-004	4.30	0.0649
B-Speed	2.223 E-004	1	2.223 E-004	3.56	0.0885
C- Depth of cut	1.022 E-004	1	1.022 E-004	1.64	0.2297
AB	1.625 E-004	1	1.625 E-004	2.60	0.1377
AC	8.845 E-005	1	8.845 E-005	1.42	0.2614
BC	5.245 E-005	1	5.245 E-005	0.84	0.3809
A2	2.170 E-005	1	2.170 E-005	0.35	0.5685
B2	1.377 E-004	1	1.377 E-004	2.20	0.1684
C2	8.052 E-005	1	8.052 E-005	1.29	0.2826
Residual	6.243 E-004	10	6.243 E-005		
Lack of fit	6.243 E-004	3	2.081 E-004		
Pure error	0.000	7	0.0000		
Cor Total	0.019	19			

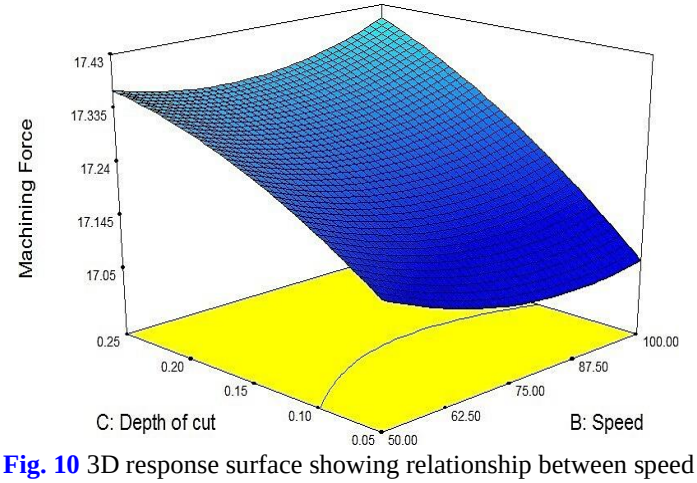

Fig. 10 3D response surface showing relationship between speed and depth of cut on machining force.

Figure 9 illustrates the impact of the feed rate and depth of cut on the machining force. According to this graph, the value of machining force rises significantly as feed rate rises and barely at all as cut depth rises. Furthermore, it is noted that the increase in machining force is mostly unrelated to the depth of cut. This figure indicates that the value of machining force increases much as the feed rate increases and very slightly as the depth of cut increases. Further, it is also observed that the depth of cut has very little contribution to the increase in Machining force. As read from the contour graph Fig. 10, the machining force value lies within when the depth of cut ranges between 0.05 and 0.25 mm and the feed rate ranges from 0.04 to 0.12 mm/rev. Also, the Machining force appears to rise while the depth of cut is between 0.15 and 0.25 mm and the feed rate are in the range of 0.04 and 0.12 mm/rev.

The Fig. 10 shows the effect of the Depth of Cut and the Speed on Machining force. From this, it is observed that the Machining force increases considerably with an increase in the cutting speed and slightly with an increase in the depth of cut. According to the contour graph, when the cutting speed is between 50 and 100 m/min and the depth of cut is between 0.05 and 0.15 mm, the machining force value is between 17.43 N. Further, it is also observed that the Machining force seems to increase consistently while the depth of cut is between 0.05 and 0.25 mm and the cutting speed is between 62.5 and 87.5 m/min.

4.1 ANN technique

It is an emerging Artificial Intelligence (AI) technique and it is utilized to test and validate the experimental data. It's general structure is as shown in Fig. 11.

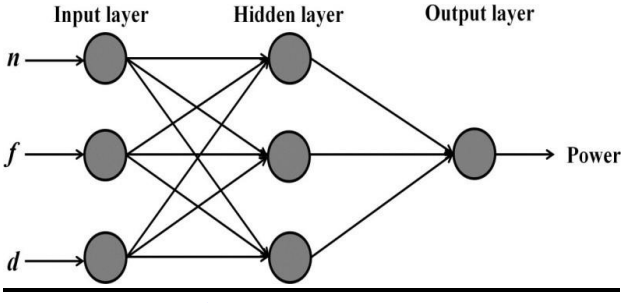

Fig. 11 ANN structure.

An artificial neural network is an information-processing system that has certain performance characteristics in common with biological neural networks.

A neural net consists of a large number of simple processing elements called neurons, units, cells or nodes. Each neuron is connected to other neurons by means of directed communication links, each with an associated weight. These weights represent information being used by the net to solve a problem. Neural nets can be applied to patterns, or finding solutions to constrained optimization problems.

Each neuron has an internal state called its activation or activity level, which is a function of the inputs it has received. Typically, a neuron sends its activation as a signal to several other neurons. It is important to note that a neuron can send only one signal at a time, although that signal is broadcast to several other neurons.

4.2 Supervised training

Perhaps in the most typical neural net setting, training is accomplished by presenting a sequence of training vectors or patterns, each with an associated target output vector. The weights are then adjusted to a learning algorithm. This process is known as supervised training.

4.3 Back propagation neural network (BPNN)

The back propagation algorithm has made it possible to design multi-layer neural networks for numerous applications, such as adaptive control, classification of sonar targets, stock market prediction and speech recognition. Also, BPNN has the advantage of fast response and high learning accuracy. One of the advantages of using the neural network approach is that a model can be constructed very easily based on the given input and output and trained to predict process dynamics accurately. This technique is especially valuable in processes where a complete understanding of the physical mechanisms is very difficult, or even impossible to acquire, as in the case of porous powder performs during upsetting. Neural network is a logical structure with multi-processing elements, which are connected through interconnection weights. The knowledge is presented by the interconnection weights, which are adjusted during the learning phase. There are several algorithms available among which the Levenberg–Marquardt algorithm (trainlm) will have the fastest convergence. In many cases, trainlm is able to obtain lower mean square errors than any of the other algorithms tested. This BP network is a multi-layer of the network architecture including the input layer, hidden layer(s) and output layer. Layers include several processing units known as neurons. They are connected with each other by variable weights to be determined. In the network, the input layer receives information from external source and passes this information to the network for processing. The hidden layer receives from the input layer, and does all information processing. The output layer receives processed information from the network, and sends the results to an external receptor. The algorithm for the back propagation program is described with the help of flow diagram as shown in Fig. 12.

4.4 Model description

In the development of a multi-layer neural network model, several decisions regarding the number of neuron(s) in the input layer, number of hidden layer(s), number of neuron(s) in the hidden layer(s), and number of neuron(s) in the output layer and optimum architectures have to be decided. Based on the experimental condition, the important input parameters, such as the helix angle, feed rate and spindle speed are given as input parameters to the present ANN model. Machining force is the output parameter.

4.5 Data normalization

In order to provide equal importance of the influence of the smaller value as like higher valued input variables, both the input and the output variables were normalized within the range of −1 to 1 before the training of the network. The normalized values (x_n) for each raw input/output dataset (d_i) were calculated as Eq. (7).

$$x_n = \frac{2(d_i - d_{min})}{(d_{max} - d_{min})} - 1 \tag{7}$$

where d_{max} and d_{min} are the maximum and the minimum values of raw data.

4.6 Neural network design

The generalization capability of the neural network is essentially dependent on (i) the selection of the appropriate input/output parameters of the system, (ii) the distribution of the dataset, and (iii) the format of the presentation of the dataset to the network. In this study, the total number of experimental results is 20 dataset among which 14 (two-third) dataset were considered for training, and 6 for testing. Before training the network, the input/output dataset were normalised within the range of ±1 using the Eq. (1). The standard multi-layer feed forward back propagation hierarchical neural networks were designed in the MATLAB 10 Neural Network Toolbox. The networks consist of three layers, namely, the input, hidden layer, and output layer. Now, the designed network has 3 input neurons and one output neuron. Initially, four neurons in input layer, 2 hidden neurons in one hidden layer and 2 neurons in output layer (3–2–1) architecture was taken and trained with 1000 epochs (iterations) to predict the optimum results. The MSE achieved from different iterations is shown in Table 1. It is evident that the value of MSE gradually decreases during the progress of training.

4.7 Neural network training

In this study, the total number of data obtained from experimental investigation is 20 set for each response among which 14 (two-third) data set were considered for training, and 6 for testing. The standard multilayer feed forward back propagation hierarchical neural networks were designed with MATLAB 10 Neural Network Toolbox. The networks consist of three layers: the input, the hidden layer, and the output layer. Now, the designed network has four input neurons and two output neurons. In the network, each neuron receives total input from all the neurons in the proceeding layer as Eq. (8):

$$net_j = \sum_i W_{ij}^n \ (X_i)^{n-1} \tag{8}$$

Where net_j is the total or net input, X_i n is the output of the node j in the nth layer, and W_{ij}^n represents the weights from node i in the (n-1) th layer to node j in the nth layer. A neuron in the network produces its input by processing the net input through an activation (transfer) function which is, usually nonlinear. There are several types of activation functions used for BP. However, the tan-sigmoid transfer function is mostly used which is assigned in hidden layer (s) for processing the inputs as Eq. (9):

$$f\ (x) = \frac{2}{(1 + e^{-x})} - 1 \ range\ (-1, 1) \tag{9}$$

The purelin, a transfer function, calculates a hidden layer's output from its net input which is assigned for output layer as

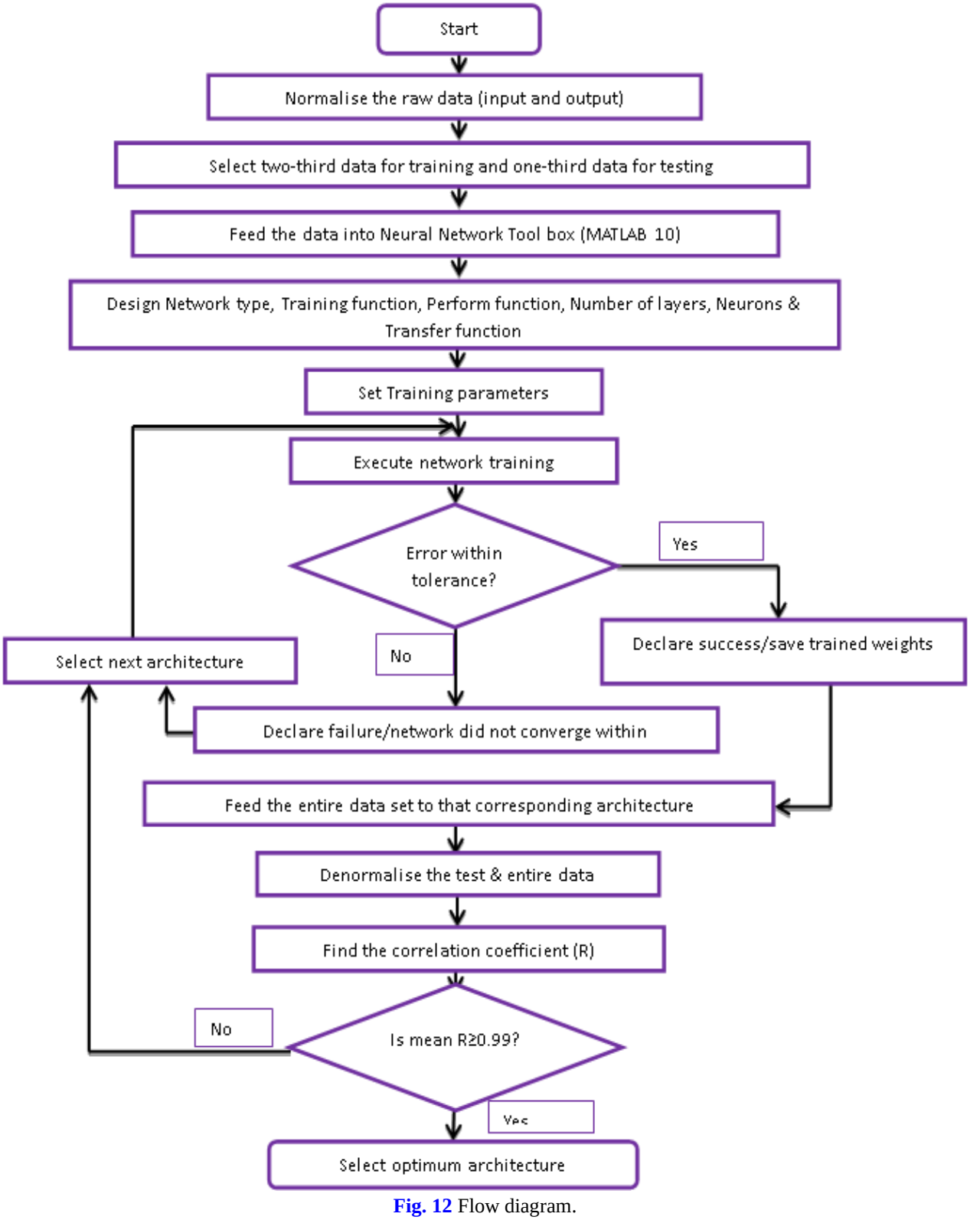

Fig. 12 Flow diagram.

Eq. (10):

$$f\,(x)\;=\;\frac{(e^{x}-e^{-x})}{(e^{x}+e^{-x})}\;-1\;range\;(-1,1) \qquad (10)$$

The weights are dynamically updated using the BP algorithm. The network has been trained with Levenberg– Marquardt algorithm. This training algorithm has been selected due to its high accuracy in similar function approximation. Default training parameters available in MATLAB 10 was set for training the dataset. In order to judge the performance of the network, the average error (MSE) has been calculated as Eq. (11):

$$E_p\;=\;\sum_{p\,=\,1}^{p}\sum_{k\,=1}^{k}\left(d_{pk}\;-\;O_{pk}\right)^2 \qquad (11)$$

In the case of BPNN training, the number of iterations (epochs) to be executed is an important parameter, which is used in the model, as presented in Table 1. To determine the best

configuration several structures, have to be considered with different numbers of hidden neurons.

The machinability of GFRP composites have been trained with different architecture by varying number of neurons in the hidden layer(s). After training, it has been demoralized and compared with the experimental data as shown in Figs. 6 and 7. The demoralized values (x_i) for each raw output dataset was calculated as Eq. (12).

$$x_i = \frac{(x_n+1)\,(d_{max}- d_{min})}{2} + d_{min} \quad (12)$$

Where d_{max} and d_{min} are the maximum and minimum values of raw data.

For testing the prediction ability of the model, prediction error in each output node has been calculated as follows Eq. (13):

$$Prediction\ error\ \% = \frac{(Actual\ value - Predicted\ value)}{Actual\ value} \times 100 \quad (13)$$

In order to determine the optimal architecture, a total of 28 different networks with different number of layers and neurons in the hidden layer have been designed and tested for GFRP composites.

4.8 Testing and performance of BPNN

The performance capability of each network has been examined based on the correlation coefficient, error distribution, and convergence of entire dataset within specified error range between the network predictions and the experimental values using the test and entire dataset. For deciding the optimum structure of neural network, the rate of error convergence was checked by changing the number of hidden neurons and number of hidden layers. In the process it had not been selected as an optimum architecture, because the mean prediction error as well as the error distribution, maximum value of error, minimum value of error were observed as high, which can be evident from Fig. 13.

4.9 Comparison of RSM and ANN models

The main advantage of RSM is its ability to exhibit the factor contributions from the coefficients in the regression model. This ability is powerful in identifying the insignificant main factors and the interaction factors or insignificant quadratic terms in the model and thereby can reduce the complexity of the problem. On the other hand, this technique requires good definition of ranges for each factor to ensure that the response(s) under consideration changes in a regular manner within this range.

It is noted that ANN models perform better than other techniques, especially RSM, when highly non-linear behavior is the case, as shown in Fig. 13. Further, this technique can build an efficient model using a small number of experiments. However, the accuracy of the technique would be better when a larger number of experiments were used to develop a model. On the other hand, the ANN model itself provides little

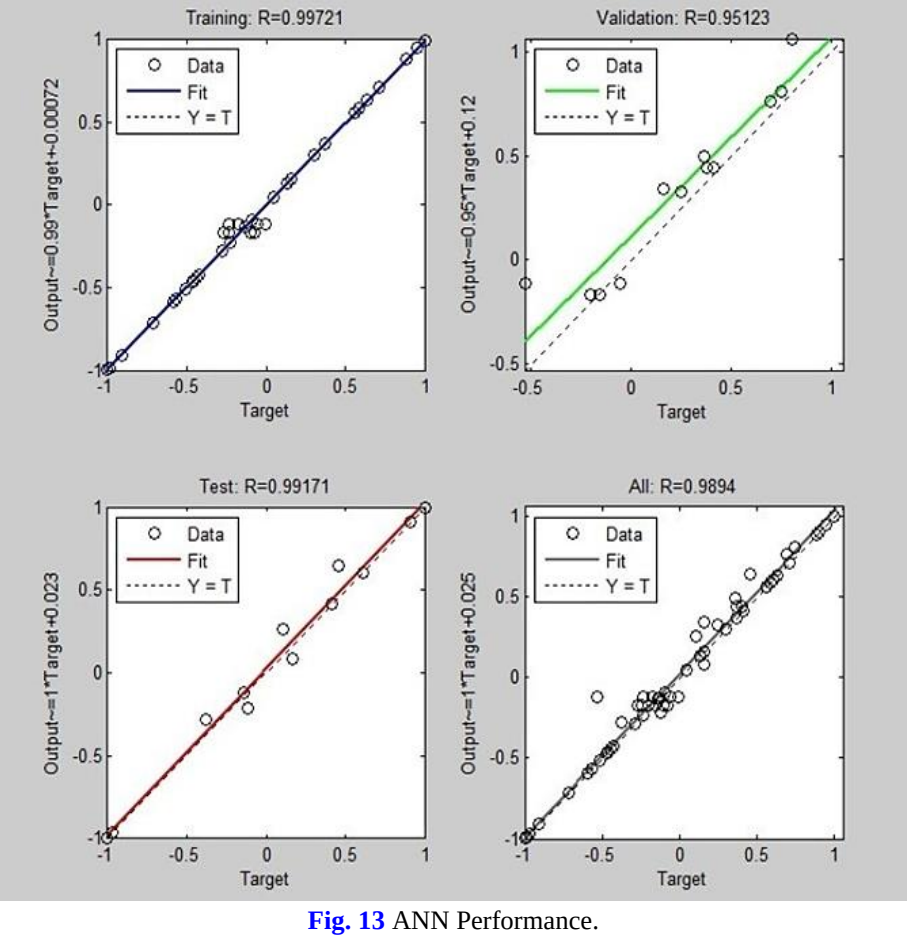

Fig. 13 ANN Performance.

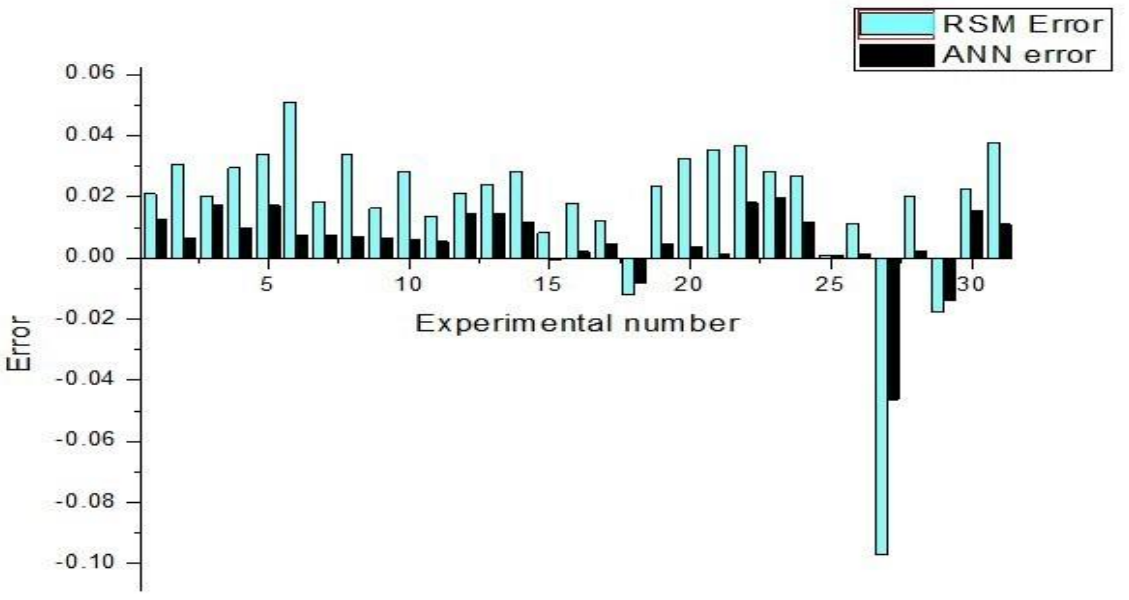

Fig. 14 comparison of RSM prediction error with ANN prediction error.

information about the design factors and their contribution to the response if further analysis has not been done.

Generation of ANN model requires a large number of iterative calculations, whereas, it is only a single step calculation for a response surface model. Depending upon the nonlinearity of the problem and the number of parameters, an ANN model may require a high computational cost to create. Although computationally much more costly than a response model, ANN model leads to comparatively accurate predictions of responses as shown in Table 6. The mean errors for ANN and RS models are about 0.258847% and 0.769831% respectively. The error against observation order of both the models is compared in Fig. 14.

Table 6. Comparison between RSM and ANN models.

Model summary and prediction errors	RSM	ANN
Mean Square Error (MSE)	6.75E-03	1.510E-3
R^2	0.97240	0.99260
Mean error/%	0.769831	0.258847
Computational time	Short	Long
Experimental domain	Regular	Irregular or regular
Model developing	With interactions	No interactions
Understanding	Easy	Moderate
Application	Frequently	Frequently

5. Conclusions

The purpose of this research is to quantify the effect of cutting speed, feed rate, and depth ofcut on machining force of GFRP composite materials. From the experimental results presented, the following conclusions were drawn from milling GFRP composite materials with solid carbide end mill tool coated with polycrystalline diamond (PCD) using response surface methodology. The Machining force tends to increase steadily with an increase in the feed rate andslightly by an increase in the cutting speed. The value of Machining force increases much as the feed rate increases and veryslightly as the depth of cut increases, which means that the composite damage is larger for higher feed rate and for higher cutting speed. The feed rate is the cutting parameter which has greater influence on Machining forcefor GFRP composite materials, followed by the cutting speed. The milling force experienced by GFRP composites was accurately anticipated by the established mathematical model. The confirmation test was used to check the created second order response surface model, and the error was found to be within 0.3%. This method makes it simple to foresee the primary effects and secondary consequences of many significant parameters. A model using Artificial Neural Networks (ANN) was developed to study the Machinability of GFRP composite during endmilling. The developed ANN model was compared with the RSM models for the prediction of machining force of milled GFRP composites. The predictive ANN model was found to be capable of better predictions of responses within the range that they had been trained. The results of the ANN model indicate it is much more robust and accurate in estimating the values of machining force when compared with the response surface model.

Conflict of Interest

There is no conflict of interest.

Supporting Information

Not applicable.

References

[1] K. J. Santosh Kumar, G. A. Bhargav, Y. Naik, K. Bommanna, Friction stir welding of different aluminum-silicon alloy

compositions utilizing conventional vertical milling machine, *Journal of Computers, Mechanical and Management*, 2022, **1**, 30-41, doi: 10.57159/gadl.jcmm.1.1.22012.
[2] G. B. Kamath, K. Subramaniam, S. Devesh, V. Chavan, N. Mohan, R. Bhat, H. T. Wijerathne, Multi-response optimization of milling process parameters for aluminium-titanium diboride metal matrix composite machining using taguchi- data envelopment analysis ranking approach, *Engineered Science*, 2022, **18**, 271-277, doi: 10.30919/es8d680.
[3] R. Kamath C, S. Bekinal, N. Naik, R. Bhat, A. Kuttan, Dynamic force modelling and experimental analysis of reaming, *Engineered Science*, 2021, **15**, 166-176, doi: 10.30919/es8e506.
[4] J. Y. Sheikh-Ahmad, Machining of Polymer Composites, Springer Science + Business Media LLC, 2009, 160-161.
[5] D. Hull, T. W. Clyne, An Introduction to Composite materials, 2 nd edition, Cambridge University press, Cambridge.
[6] J. Ramkumar, S. Aravindan, S. K. Malhotra, R. Krishnamurthy, An enhancement of the machining performance of GFRP by oscillatory assisted drilling, *The International Journal of Advanced Manufacturing Technology*, 2004, **23**, 240-244, doi: 10.1007/s00170-003-1660-8.
[7] G. B. Kamath, K. Subramaniam, S. Devesh, V. Chavan, N. Mohan, R. Bhat, H. T. Wijerathne, Multi-response optimization of milling process parameters for aluminium-titanium diboride metal matrix composite machining using taguchi- data envelopment analysis ranking approach, *Engineered Science*, 2022, **18**, 271-277, doi: 10.30919/es8d680.
[8] R. Bhat, N. Mohan, S. Sharma, S. Rao, Influence of seawater absorption on the hardness of glass fiber/polyester composite, *Journal of Computers, Mechanical and Management*, 2022, **1**, 1-11, doi: 10.57159/gadl.jcmm.1.1.22003.
[9] M. Ramulu, C. W. Wern, J. L. Garbini, Effect of fibre direction on surface roughness measurements of machined graphite/epoxy composite, *Composites Manufacturing*, 1993, **4**, 39-51, doi: 10.1016/0956-7143(93)90015-z.
[10] P. S. Sreejith, R. Krishnamurthy, S. K. Malhotra, K. Narayanasamy, Evaluation of PCD tool performance during machining of carbon/phenolic ablative composites, *Journal of Materials Processing Technology*, 2000, **104**, 53-58, doi: 10.1016/s0924-0136(00)00549-5.
[11] Y. Sahin, A. R. Motorcu, Surface roughness prediction model in machining of carbon steel by PVD coated cutting tools, *American Journal of Applied Sciences*, 2004, **1**, 12-17, doi: 10.3844/ajassp.2004.12.17.
[12] G, Santhanakrishnan, Machinability characteristics of fibre reinforced plastics composites, *Journal of Mechanical Working Technology*, 1988, **17**, 195-204, doi: 10.1016/0378-3804(88)90021-6.
[13] J. Paulo, Davim, A new machinability index in turning fiber reinforced plastics, *Journal of Materials Processing Technology*, 2005, **170**, 436-440, doi: 10.1016/j.jmatprotec.2005.05.047.
[14] K. Palanikumar, L. Karunamoorthy, R. Karthikeyan, Assessment of factors influencing surface roughness on the machining of glass fiber-reinforced polymer composites, *Materials & Design*, 2006, **27**, 862-871, doi: 10.1016/j.matdes.2005.03.011.
[15] N. Bhatnagar, N. Ramakrishnan, N. K. Naik, R. Komanduri, On the machining of fiber reinforced plastic (FRP) composite laminates, *International Journal of Machine Tools and Manufacture*, 1995, **35**, 701-716, doi: 10.1016/0890-6955(95)93039-9.
[16] Y. Sahin, A. R. Motorcu, Surface roughness prediction model in machining of carbon steel by PVD coated cutting tools, *American Journal of Applied Sciences*, 2004, **1**, 12-17, doi: 10.3844/ajassp.2004.12.17.
[17] J. P. Davim, P. Reis, C. C. António, A study on milling of glass fiber reinforced plastics manufactured by hand-lay up using statistical analysis (ANOVA), *Composite Structures*, 2004, **64**, 493-500, doi: 10.1016/j.compstruct.2003.09.054.
[18] P. P. Raj, A. Elaya Perumal, Taguchi Analysis of surface roughness and delamination associated with various cemented carbide K10 end Mills in milling of GFRP, *Journal of Engineering Science and Technology Review*, 2010, **3**, 58-64, doi: 10.25103/jestr.031.11.
[19] A. I. Khuri, 12 Multiresponse surface methodology, Handbook of Statistics. Amsterdam: Elsevier, 1996, 377-406, doi: 10.1016/s0169-7161(96)13014-5.
[20] G. Derringer, R. Suich, Simultaneous optimization of several response variables, *Journal of Quality Technology*, 1980, **12**, 214-219, doi: 10.1080/00224065.1980.11980968.
[21] J. J. Pignatiello JR, Strategies for robust multiresponse quality engineering, *IIE Transactions*, 1993, **25**, 5-15, doi: 10.1080/07408179308964286.
[22] S.-O. An, E.-S. Lee, S.-L. Noh, A study on the cutting characteristics of glass fiber reinforced plastics with respect to tool materials and geometries, *Journal of Materials Processing Technology*, 1997, **68**, 60-67, doi: 10.1016/s0924-0136(96)02534-4.
[23] F. Mata, J. P. Davim, An investigation about the precision turning fiber reinforced plastics (FRP's) with diamond cutting tools using multiple analysis regression, TRIB2003, II Iberian Conference of Tribology, Valencia, 2005, 117– 124.
[24] K. Palanikumar, Studies on machining characteristics of glass fiber reinforced polymer composites, PhD thesis, Anna University, Chennai, India, 2004.
[25] G. V. G. Rao, P. Mahajan, N. Bhatnagar, Micro-mechanical modeling of machining of FRP composites - Cutting force analysis, *Composites Science and Technology*, 2007, **67**, 579-593, doi: 10.1016/j.compscitech.2006.08.010.
[26] G. Kant, V. Rao V, K. S. Sangwan, Predictive modeling of turning operations using response surface methodology, *Applied Mechanics and Materials*, 2013, **307**, 170-173, doi: 10.4028/www.scientific.net/amm.307.170.
[27] N. Altan Özbek, O. Özbek, F. Kara, Statistical analysis of the effect of the cutting tool coating type on sustainable machining parameters, *Journal of Materials Engineering and Performance*, 2021, **30**, 7783-7795, doi: 10.1007/s11665-021-06066-8.
[28] M. Akgün, F. Kara, Analysis and optimization of cutting tool coating effects on surface roughness and cutting forces on turning of AA 6061 alloy, *Advances in Materials Science and*

Engineering, 2021, **2021**, 1-12, doi: 10.1155/2021/6498261.
[29] E. Nas, O. Özbek, F. Bayraktar, F. Kara, Experimental and statistical investigation of machinability of AISI D2 steel using electroerosion machining method in different machining parameters, *Advances in Materials Science and Engineering*, 2021, **2021**, 1-17, doi: 10.1155/2021/1241797.